Araştırma Makalesi *BAUN Fen Bil. Enst. Dergisi, 27(1), 324-341, (2025)*

DOI:10.25092/baunfbed. 1597359 *J. BAUN Inst. Sci. Technol., 27(1), 324-341, (2025)*

Investigation of the effects of fabric structural parameters on the roughness of coated fabrics

Mine AKGUN, Gizem MANASOGLU*, Mehmet KANIK

Bursa Uludag University, Faculty of Engineering, Department of Textile Engineering, Görükle Campus, Bursa.

Geliş Tarihi (Received Date): 06.12.2024
Kabul Tarihi (Accepted Date): 31.12.2024

Abstract

In this study, the effects of the weave structures used in the base fabric on the surface roughness parameters of coated polyester fabrics were investigated. 100% polyester fabrics woven with different weft yarn densities in the basket, twill, and sateen weave patterns were coated with calcite ($CaCO_3$), a widely used and economical filler in the textile coating. The surface properties of the fabrics were examined by evaluating various surface roughness parameters such as arithmetic average height (R_a), mean height of peaks (R_{pm}), and mean depth of valleys (R_{vm}). Warp yarn properties were kept constant to investigate the effect of changes in weave pattern and weft yarn density. Experimental results indicated that surface roughness values changed depending on the weave pattern of the base fabric, warp and weft directions, and weft yarn density. Overall, after the coating process, the R_a, R_{pm}, and R_{vm} values decreased in both the weft and warp directions.

Keywords: *Coating, weave pattern, surface roughness, polyester.*

Kumaş yapısal parametrelerinin kaplanmış kumaşların pürüzlülüğü üzerindeki etkilerinin araştırılması

Öz

Bu çalışmada kaplamalı polyester kumaşların yüzey pürüzlülük parametreleri üzerine zemin kumaşta kullanılan dokuma yapısının etkisi incelenmiştir. Panama, dimi ve saten örgü yapılarında farklı atkı ipliği sıklıkları ile dokunan %100 polyester kumaşlar tekstil kaplamacılığında yaygın olarak kullanılan ve ekonomik bir dolgu maddesi olan kalsit ($CaCO_3$) ile kaplanmıştır. Kumaşların yüzey özellikleri, aritmetik ortalama yükseklik

* Gizem MANASOGLU, gmanas@uludag.edu.tr, https://orcid.org/0000-0002-1504-8694

(R_a), ortalama tepe yüksekliği (R_{pm}) ve ortalama vadi derinliği (R_{vm}) gibi çeşitli yüzey pürüzlülük parametreleri değerlendirilerek incelenmiştir. Örgü deseni ve atkı ipliği sıklığındaki değişimin etkisini incelemek amacıyla çözgü ipliği özellikleri sabit tutulmuştur. Deneysel sonuçlar, yüzey pürüzlülük değerlerinin zemin kumaşının desenine, çözgü ve atkı yönlerine ve atkı ipliği sıklığına bağlı olarak değiştiğini ve genel olarak kaplama işleminden sonra R_a, R_{pm} ve R_{vm} değerlerinin hem atkı hem de çözgü yönünde azaldığını göstermiştir.

Anahtar kelimeler: *Kaplama, dokuma deseni, yüzey pürüzlülüğü, polyester.*

1. Introduction

Textile surfaces that have improved performance properties via coating and lamination techniques have many uses, such as clothing, agriculture, medical, construction, geotextile, home textiles, industrial textiles, protective clothing, packaging, sports, automotive, and so on [1]. Coating fabrics are composite materials created by applying a polymer coating material to one or both surfaces of the fabric in one or multiple layers. The polymer coating provides the fabric with some new functional properties, as well as improving its physical properties, such as abrasion resistance. Fabric components mostly impart integrity to the system. They often dominate the strength of coated/laminated fabrics and generally determine tear and tensile strength, elongation, and dimensional stability [1,2]. The polymeric layer provides various desired properties to textiles, including resistance to penetration and impermeability to liquids, gases, and dust particles, increased conductivity, shielding from electromagnetic interference/radio frequency interference, and modification of appearance for decorative purposes [3]. The nature of the layers (fabric/polymer) and their combined characters determine the general properties of the coated sample. The final product will have many features that the components cannot offer individually. Therefore, it is important to carefully evaluate and select the base fabric and coating polymer to ensure the desired outcome [1,4].

Calcite is the term generally used for industrial minerals, which are defined as crystallized calcium carbonate ($CaCO_3$) [4]. It is a naturally occurring substance and forms in various crystal shapes, including rhombohedral and scalenohedral. It can be easily ground into a fine white powder and is widely used as a filler in industries such as paint, paper, plastic, coatings, composites, textiles, printing inks, and pharmaceutical products due to its whiteness, low cost, negligible toxicity, and beneficial features [4-10]. It remains chemically stable up to 800 °C [11]. Calcium carbonate particles show good compatibility with many organic and inorganic matrices [12]. Therefore, they were utilized in various studies to enhance mechanical performance, thermal resistance, stability, and hydrophobicity [8, 13-15]. For instance, Yang et al. examined epoxy composites produced with different amounts of rod-like and cube-like $CaCO_3$ nanoparticles, focusing on their thermal stability and mechanical properties. They found that the presence of $CaCO_3$ significantly improved the mechanical properties, such as the flexural strength and modulus, compared to pure epoxy. Both forms of calcite enhanced the thermal stability of the composites relative to the reference material. Notably, the epoxy composites containing rod-like $CaCO_3$ exhibited higher char yields at 800°C [16]. Wu et al. examined the impact of in-situ deposition of nano-$CaCO_3$ on the properties of anti-creasing cotton fabrics. The treatment increased the breaking strength of the fabrics by approximately 11–14 % without significant change in their wrinkle recovery angle [17].

Stambouli et al. investigated the effect of calcium carbonate in improving the thermal property of PVC foamed layer used for coated textiles. The melting point and the onset decomposition temperatures of the $CaCO_3$-filled foamed layer increased compared with the unfilled PVC. Additionally, it was observed that using smaller-sized calcium carbonate particles enhanced the thermal stability even further [18]. Abeywardena et al. applied surface-modified superhydrophobic precipitated calcium carbonate particles (SHPCC) onto polyester fabrics using the dip coating method. Their findings indicated that the wetting properties of the coated surfaces decreased as the calcium carbonate concentration increased. The highest water contact angle of 150.2° was achieved with a 6% concentration of SHPCC [19]. In another study, Hou et al. studied the effect of hydrophobic modified calcium carbonate nanoparticles on the properties of the polyvinylidene fluoride (PVDF)/nonwoven fabric flat-sheet composite membranes. It was indicated that incorporating nanoparticles into the PVDF matrix increased the surface roughness, contact angle, and crystallinity values of the membranes [20].

Surface roughness is a measure of the surface texture [21]. It is often described as uneven, irregular, and coarse in texture. Surface roughness plays an important role in various applications that involve friction, lubrication, and wear. In general, it is observed that friction increases with increased average roughness. Therefore, roughness parameters are substantial in applications such as on surfaces subject to friction. In literature, a correlation is found between the initial roughness of sliding surfaces and their wear rate. Such correlations can be used to predict the failure time of contact surfaces. Also, surface roughness plays an important role in contact resistance. Thermal or electrical conduction between two surfaces in contact occurs only through certain regions [22].

Fabrics containing more peaks and lower amplitude pulses are defined to be smoother than those with fewer peaks and higher amplitudes. In general, fabric surfaces have two kinds of irregularities; systematic variation arising from uniform fabric structures such as weave patterns and random variations caused by uneven threads or thread spacing [23]. Fabric surface properties are closely related to yarn count, yarn density, and weave pattern. The value of the yarn spacing is highly dependent on the linear density of yarns and weave structure. It also defines the intensity of the effect of certain yarns on the fabric surface and leads to an increase in the intensity of relief. At a warp and weft yarn interlacing point, the location of the yarns changes between the face and the back of the fabric. Yarns pass through the spaces between the yarns of the other yarn system and contact them over a large surface area. In a plain weave possible to achieve the lowest value of yarn spacing due to the frequent changes in the position of warp and weft yarns. In the weaves with slightly larger repeats, however, it is possible to practically achieve a higher number of yarns per unit length, as the change of yarns from face to backside or vice versa occurs less frequently (twills and satins of smaller repeats) [24]. Generally, a plain weave exhibits a higher geometric roughness than a twill weave due to its shorter floats [25].

As the number of threads per unit length in the fabric increases, the fabric surface becomes smoother because of the decrease in the yarn crown heights due to the increased yarn sett. An increase in yarn diameter also increased the fabric surface roughness. The increase in surface roughness was ascribed to an increase in mechanical intersecting of yarn crowns [26]. The structural parameters forming the woven fabrics affect the surface roughness values. Fabrics with high yarn density could have a compact structure due to small porosity values between yarns in the fabric structure [27]. The closeness of yarns in fabric structure decreases differences between high and low peaks on the fabric surface, and as a result, fabric surface roughness decreases [27, 28]. Similar to these results, in another study examining the effect of weft yarn density and weave patterns on surface roughness, it was indicated that samples with low yarn intersection and low weft yarn density gave the highest roughness values and were, therefore, more affected by the abrasion [29]. It was also stated in the literature that the surface roughness properties of polyester fabrics were affected by the balance and cover factor of the fabric and that these effects were related to the fabric thickness, yarn densities, yarn crimp, and the placement of the yarns in the fabric structure. It was stated that a change in weave pattern from sateen to plain and, similarly, an increase in weft yarn density increased the fabric balance and decreased the fabric surface roughness [28].

The surface roughness values of the samples decreased as the fabric cover factor increased for the same weave structure. However, for the fabrics with different weave patterns, it was also shown that different surface roughness values were obtained in fabrics with the same cover factor. When calculating the fabric cover factors according to the yarn densities and counts, the weave patterns are not considered [30]. So, the findings revealed that the roughness changed significantly depending on the positioning of the yarns in the fabric, as well as the yarn density [28].

In this study, the effect of the weave pattern of the base fabric on the surface roughness properties of coated fabrics was investigated in both warp and weft directions and for different weft yarn densities under constant coating process conditions. Changes in the fabric surface roughness parameters after coating were evaluated by scanning electron microscope and optical visual analysis of the fabric surfaces and by correlating them with changes in fabric thickness and mass per unit area values.

2. Materials and methods

2.1. Material

Base fabrics woven with %100 polyester texturized yarns in different weave patterns and different weft yarn densities were used. The constructional parameters of the fabrics are presented in Table 1.

To assess the impact of the weave structure on the surface roughness of coated fabric, the 3/3 basket, 1/3 twill, and 1/5 sateen weave structures were utilized. The weave patterns are illustrated in Figure 1.

Table 1. Constructional parameters of fabrics.

Weave Pattern	Yarn Density (thread/cm)		Yarn Count (denier/filaments)	
	Warp	Weft	Warp	Weft
3/3 Basket	30	24	300/96	300/96
	30	30	300/96	300/96
1/3 Twill	30	24	300/96	300/96
	30	30	300/96	300/96
1/5 Sateen	30	24	300/96	300/96
	30	30	300/96	300/96

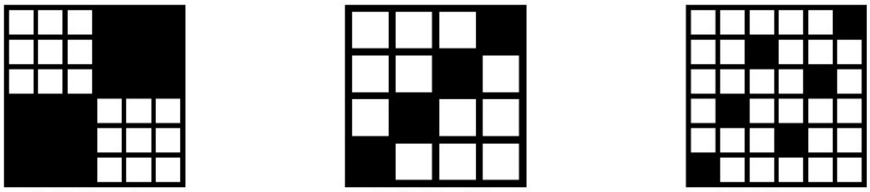

Figure 1. Weave patterns of fabrics.

The calcite powder used as filler material in the coating had a particle size of 5.5 ± 0.5 microns. It was supplied by Aydın Mining (Bursa). The other coating chemicals included the acrylic binder (AC 111), thickener (Ruco-Coat TH 5020), fixation agent (Ruco-Coat FX 8011), and the anti-foam agent (Ruco-Coat DA 3000), were provided by Rudolf Duraner (Bursa).

2.2. Methods

During the preparation of the pastes, the basic coating chemicals were combined using a high-speed mechanic stirrer. In the controlled and slow addition of thickener, the mixing speed was increased to approximately 2500 rpm. After adding the calcite powder, the viscosity was measured with a Brookfield RVT viscometer, and the remaining portion specified in the recipe was adjusted with either water or additional thickener to achieve the desired viscosity, which was set at 7000 ± 200 centipoises. The coating paste recipe provided in Table 2 shows the amounts of each chemical used.

Table 2. Coating paste recipe.

Chemical	Content (g)
Binder	280
Ammonia	5
Fixation agent	16
Anti-foam agent	12
Synthetic thickener	16
Calcite powder	100
Water	571
Total	1000

Woven fabrics were coated on the Ataç GK 40 RKL laboratory-type machine according to the knife-over-roll method. The coating was applied to the weft-faced side of the fabrics in the warp direction. The distance between the knife and fabric was arranged as 0.5 mm for all samples. Coated fabrics were dried at 100˚C for 10 minutes in the same machine. Then, samples were cured using a Rapid HT Steamer at a temperature of 160˚C for 3 minutes, following the hot air-drying principle.

The mass per unit area and thickness of fabrics were measured according to ASTM D3776 and ASTM D1777-96 standards, respectively [31, 32]. Optical images of both uncoated and coated samples were captured using a microscope equipped with a digital camera (Mshot, MS60) with a magnification rate of 45X. This was done to observe the fabric surfaces in relation to various construction parameters. Surface images of the fabrics were obtained under both top and bottom illumination to analyze the peaks and valleys of the fabric surfaces, as well as their porosity. Additionally, scanning electron microscope

(SEM) images of the coated fabrics were taken using a Zeiss EVO 40 microscope at a magnification rate of 100X.

The surface roughness measurements of fabrics were carried out in Surfcom 130A surface roughness tester according to the ISO 21920-2:2021 [21] standard. The surface roughness of uncoated and coated fabric samples was measured in both the warp and weft directions, with five measurements taken from each sample to obtain average values. The measurements were carried out at a sample length of 50 mm and a measurement speed of 1.5 mm/sec. For the characterization of fabric surface roughness, arithmetic average height (R_a), mean height of peaks (R_{pm}), and mean depth of valleys (R_{vm}) were selected.

R_a is the arithmetical average of absolute values of the profile variations between peaks and valleys from the mean line in the evaluation length. R_{pm} and R_{vm} are defined as the mean of the maximum height of peaks and the mean of the maximum depth of valleys obtained for each sampling length of the evaluation length, respectively [33].

3. Results and discussion

3.1. Evaluation of changes in thickness and mass per unit area after coating process

Table 3 presents the mass per unit area and thickness values of the fabrics before and after coating, along with the percentage increases in these values after coating.

Table 3. Mass per unit area and thickness results.

Weave Pattern	Weft Yarn Density (thread/cm)	Mass per Unit Area (g/m^2)			Thickness (mm)		
		Uncoated	Coated	Increase (%)	Uncoated	Coated	Increase (%)
3/3 Basket	24	278	399	43.53	0.70	0.78	12.36
	30	294	404	37.41	0.63	0.69	10.03
1/3 Twill	24	271	380	40.22	0.65	0.68	4.96
	30	302	413	36.75	0.64	0.67	4.39
1/5 Sateen	24	250	379	51.60	0.69	0.73	5.64
	30	282	408	44.68	0.64	0.70	9.23

It was observed that the mass per unit area of all fabrics increased after the coating process. Due to the amount of solid material transferred to the fabrics, it was an expected result and aligned with literature examples [34-36]. As seen in Table 3, the increases were lower in fabrics with high weft yarn density. This result was attributed to the fact that an increased weft yarn density results in more yarns per unit area, making the fabric more compact and reducing the gaps between the yarns (Figures 2-4). Consequently, the filling of the coating material into the gaps between the yarns was reduced. When examining the changes in fabric thickness values presented in Table 3, it was noted that the thickness of all fabrics increased after the coating process.

After the water contained in the paste evaporates during drying, a solid coating film remains on the fabric surface, and as an expected result, the thickness value increases compared to the state before the coating [37].

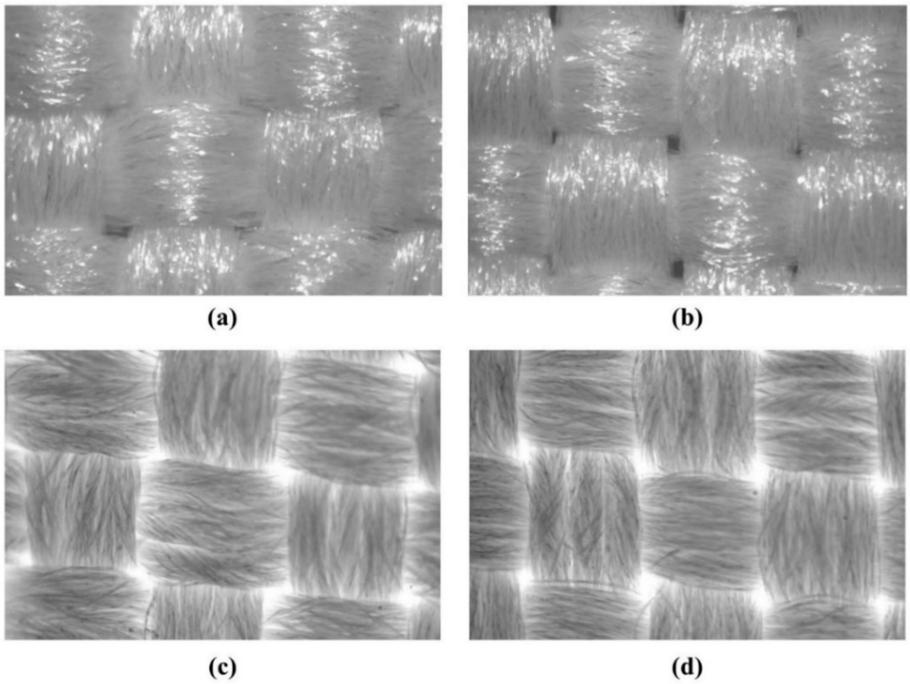

Figure 2. Optical images of basket weave uncoated fabrics (Mag: 45X). (a) 24 weft/cm, top illumination (b) 30 weft/cm, top illumination (c) 24 weft/cm, bottom illumination (d) 30 weft/cm, bottom illumination

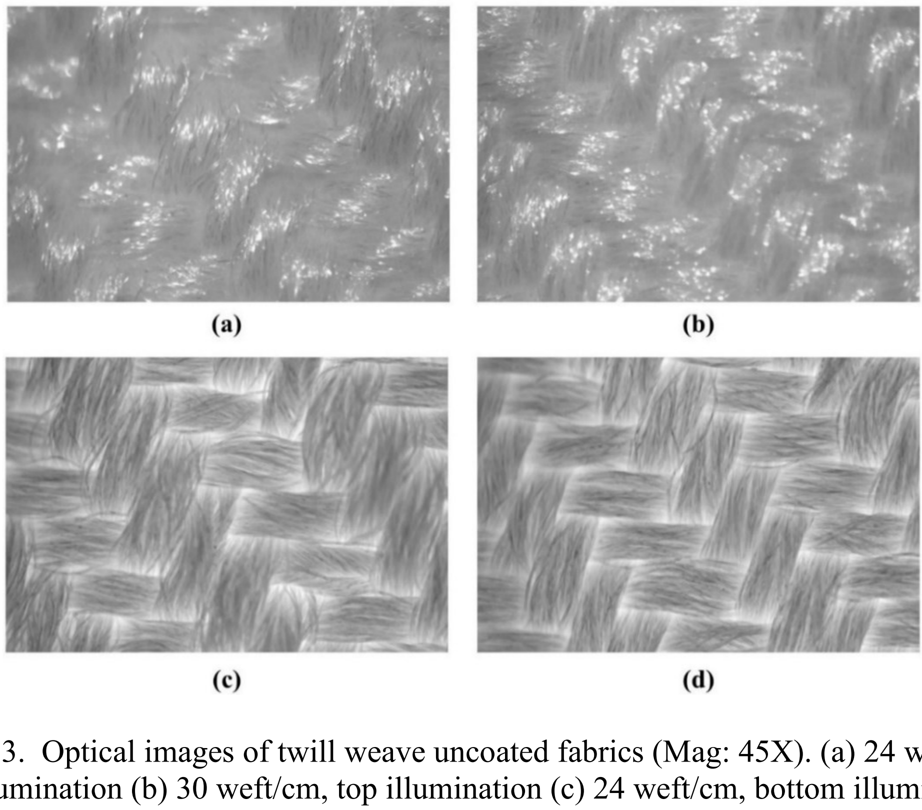

Figure 3. Optical images of twill weave uncoated fabrics (Mag: 45X). (a) 24 weft/cm, top illumination (b) 30 weft/cm, top illumination (c) 24 weft/cm, bottom illumination (d) 30 weft/cm, bottom illumination

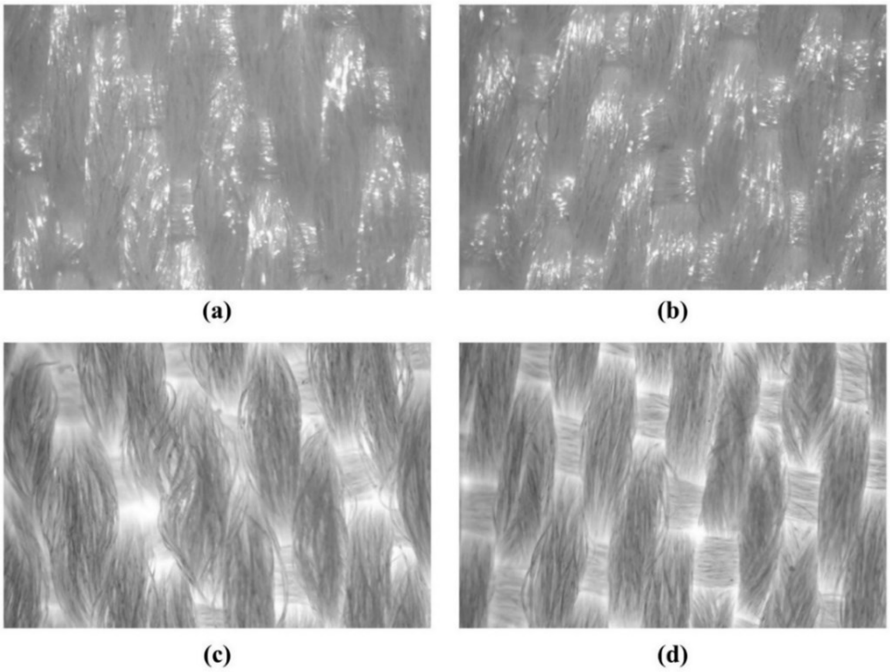

Figure 4. Optical images of sateen weave uncoated fabrics (Mag: 45X). (a) 24 weft/cm, top illumination (b) 30 weft/cm, top illumination (c) 24 weft/cm, bottom illumination (d) 30 weft/cm, bottom illumination

The fabric with a 3/3 basket weave structure exhibited the highest increase in thickness following the coating application (Figure 2). It was considered that this result might be due to the crimp peaks formed on the surface of the fabric due to the intersection of the threads in the 3/3 basket weave structure in groups of three. This might contribute to a higher increase in thickness after coating (Figure 5 and Figure 6).

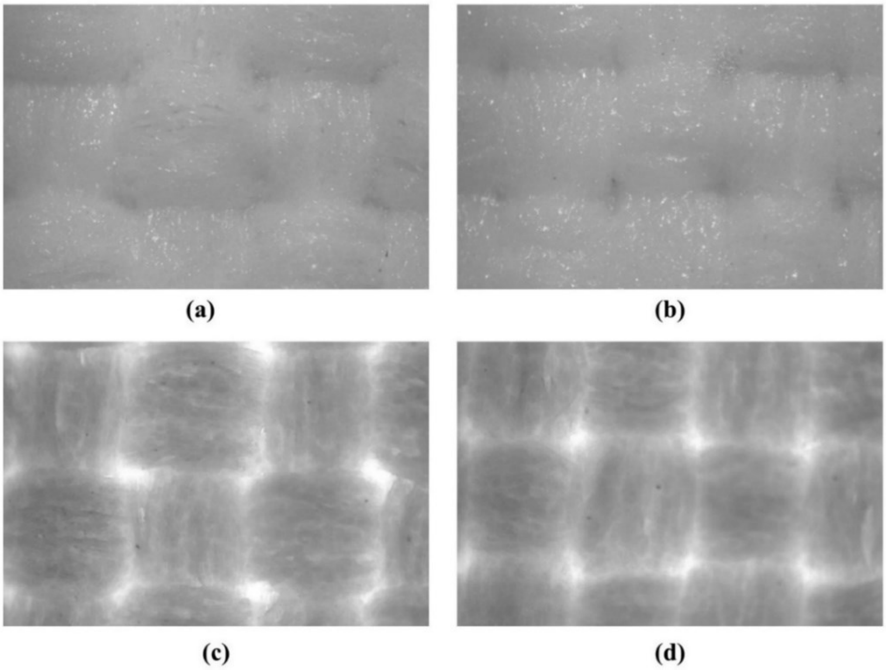

Figure 5. Optical images of basket weave coated fabrics (Mag: 45X). (a) 24 weft/cm, top illumination (b) 30 weft/cm, top illumination (c) 24 weft/cm, bottom illumination (d) 30 weft/cm, bottom illumination

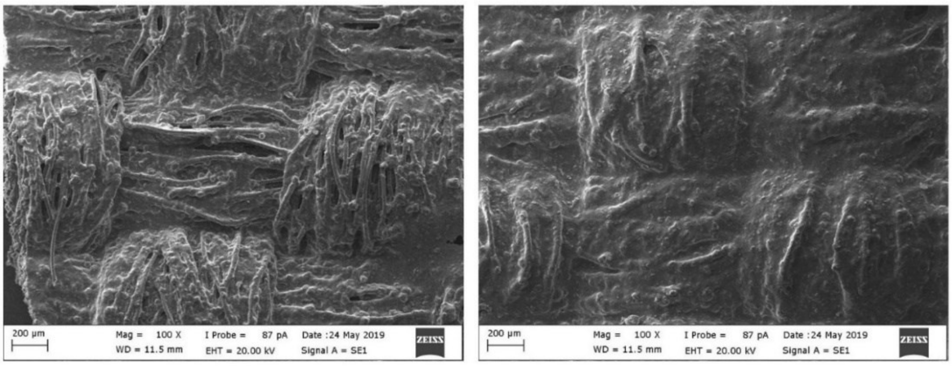

(a) (b)

Figure 6. SEM images of basket weave coated fabrics (Mag: 100X).
(a) 24 weft/cm, top illumination (b) 30 weft/cm, top illumination

It was seen that the lowest fabric thickness increase after the coating process was in the fabric with a 1/3 twill weave structure. It was thought that this outcome was due to the presence of diagonal channels on the surface of the twill weave (Figure 3). These channels prevented a significant increase in thickness by filling with the coating material (Figure 7 and Figure 8).

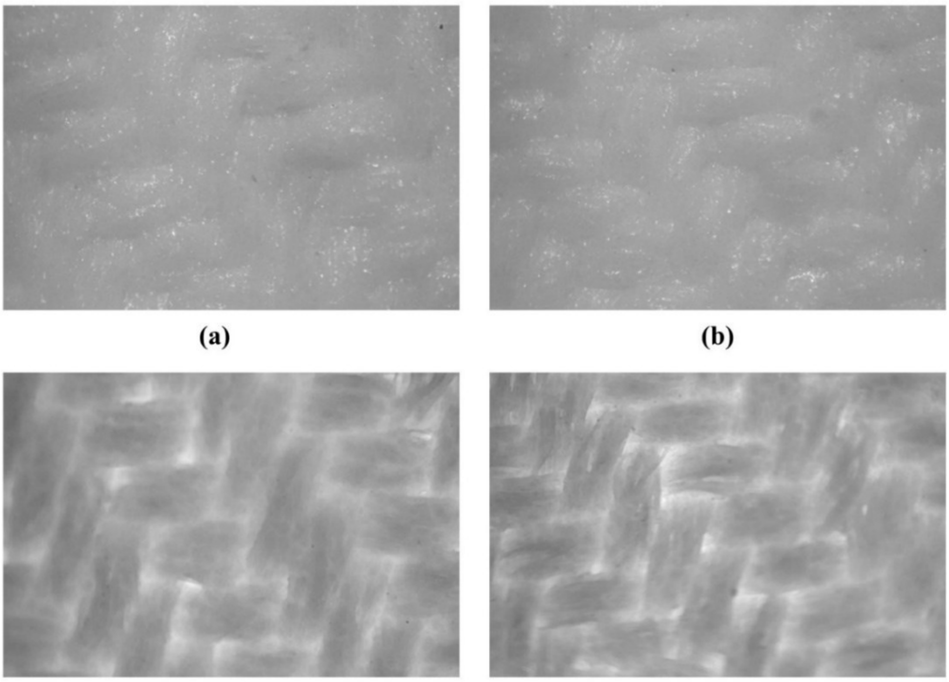

(a) (b) (c) (d)

Figure 7. Optical images of twill weave coated fabrics (Mag: 45X). (a) 24 weft/cm, top illumination (b) 30 weft/cm, top illumination (c) 24 weft/cm, bottom illumination (d) 30 weft/cm, bottom illumination

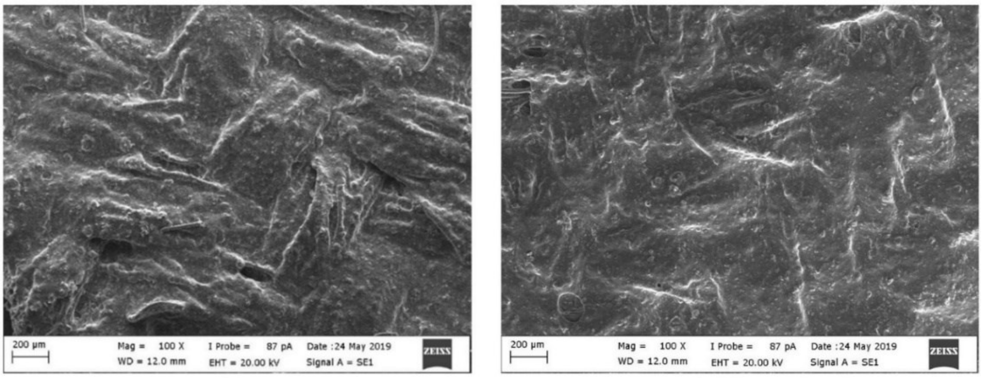

(a) **(b)**

Figure 8. SEM images of twill weave coated fabrics (Mag: 100X).
(a) 24 weft/cm, top illumination (b) 30 weft/cm, top illumination

It was observed that the base fabric, which had a 1/5 sateen weave structure, had a different tendency compared to the other fabrics examined. Namely, the % increase in fabric thickness in 3/3 basket and 1/3 twill fabrics was lower due to the increase in the weft density of the fabric. However, in the fabric structure where sateen weave was used on the base, the increase in fabric thickness was 5.64% at low weft yarn density, while it was 9.23% at high weft yarn density. This situation suggested that the sateen structured base fabric, where the long floating yarns on the fabric surface (Figure 4), also increased the weft yarn density per unit area, and as a result, the coating applied to the fabric surface increased the fabric thickness by causing it to remain on the surface in higher amounts (Figure 9 and Figure 10).

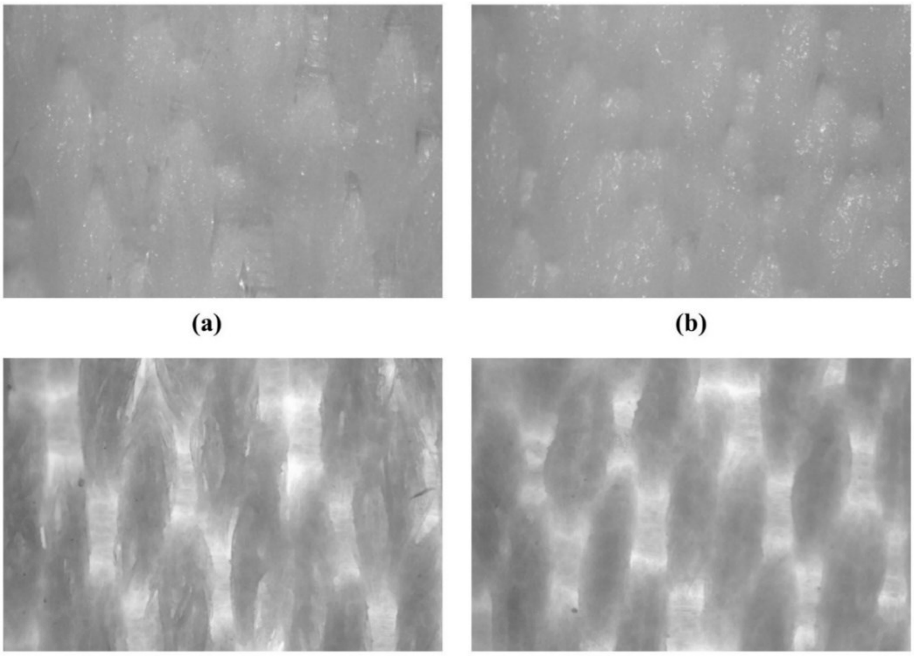

(c) **(d)**

Figure 9. Optical images of sateen weave coated fabrics (Mag: 45X). (a) 24 weft/cm, top illumination (b) 30 weft/cm, top illumination (c) 24 weft/cm, bottom illumination (d) 30 weft/cm, bottom illumination

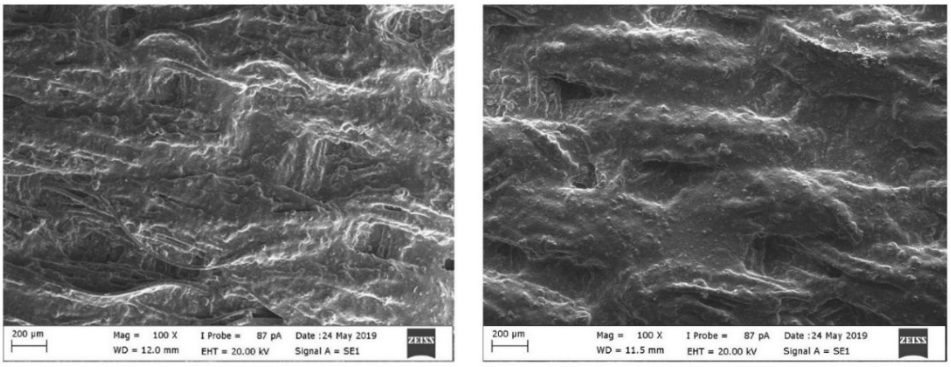

(a) **(b)**

Figure 10. SEM images of sateen weave coated fabrics (Mag: 100X).
(a) 24 weft/cm, top illumination (b) 30 weft/cm, top illumination

3.2. Evaluation of the fabric surface roughness parameters in warp direction

The effects of weave and weft yarn densities on the R_a values of uncoated and coated fabrics in the warp direction are given in Figure 11. It was observed that among the uncoated fabrics, the basket weave exhibited the highest R_a values, indicating greater surface roughness, while the sateen weave showed the lowest R_a values. The basket weave was followed by twill and then sateen weave structures. The R_a value of the basket weave was higher than that of the other weave structures because the yarns move in three groups and create intersections (Figure 2). The sateen weave structure had long yarn floats on the fabric surface and also did not have any orientation effect as in twill weave (Figure 3). As a result of this it was considered that the R_a values of the sateen fabric surface were found to be lower (Figure 4).

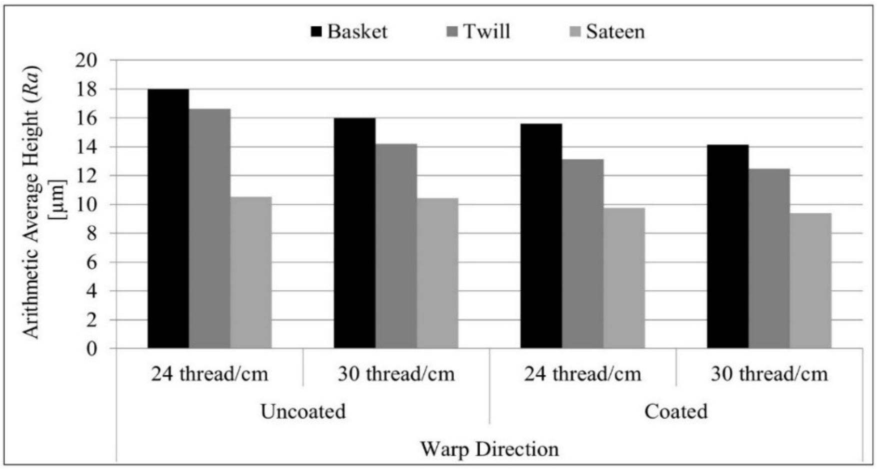

Figure 11. Changes of the arithmetic average height (R_a) values of fabrics in the warp direction.

When examining the impact of weave structures on the R_a values of the fabric after the coating process in the warp direction, it was found that the sateen weave (Figure 9 and Figure 10) used as the base fabric resulted in the lowest R_a value. The highest R_a value was observed in the basket weave (Figure 5 and Figure 6). Overall, the R_a values of samples decreased from the basket weave structure to the twill and sateen weave structure.

When the changes in warp direction R_a values of fabrics after coating were examined for weft densities of 24 and 30 threads/cm, respectively, R_a values decreased by approximately 13.39% and 11.50% in basket weave, 20.97% and 12.21% in twill weave, 7.43% and 9.94% in sateen weave.

The smallest change in the R_a values occurred in the sateen base fabric after the coating process. The most significant change occurred in the twill base fabric, which had a low weft yarn density. It was thought that this result was due to the effect of the diagonal orientation of the yarns in the twill weave structure. The coating process greatly reduced this diagonal effect of the surface (Figure 7 and Figure 8).

R_a values on the warp direction decreased as the weft yarn density increased. Figure 11 illustrates that an increase in weft yarn density leads to a more significant reduction in R_a values for fabrics with basket and twill weave structures. The decrease in R_a value for the sateen weave structure was lower with the increased weft yarn density. The reduction in R_a values was more substantial in fabric structures that initially exhibited high roughness values, such as those with basket and twill weaves. As a result, it could be possible to reduce the R_a values by increasing the weft yarn density of a fabric structure having a high R_a value.

It was seen that the change in weft yarn density had a significant effect on the roughness values of fabrics. This was because when the stylus of the measuring device moved in the warp direction, it was affected by the properties of the weft yarn and the variations in the weft yarn densities to which the warp yarns were connected. When the weft yarn density was low, the distance between the two weft yarns was higher. Conversely, as the weft yarn density was increased, the gap between the two weft yarns would decrease. This reduction in the gaps between two consecutive yarns would lead to a decrease in the amplitude of peaks and valleys on the fabric surface, resulting in a smoother texture.

The impact of changes in fabric weave and weft yarn density on the uncoated and coated surfaces on the mean height of peak (R_{pm}) and mean depth of valley (R_{vm}) values in the warp direction of the fabrics are given in Figure 12 and Figure 13, respectively.

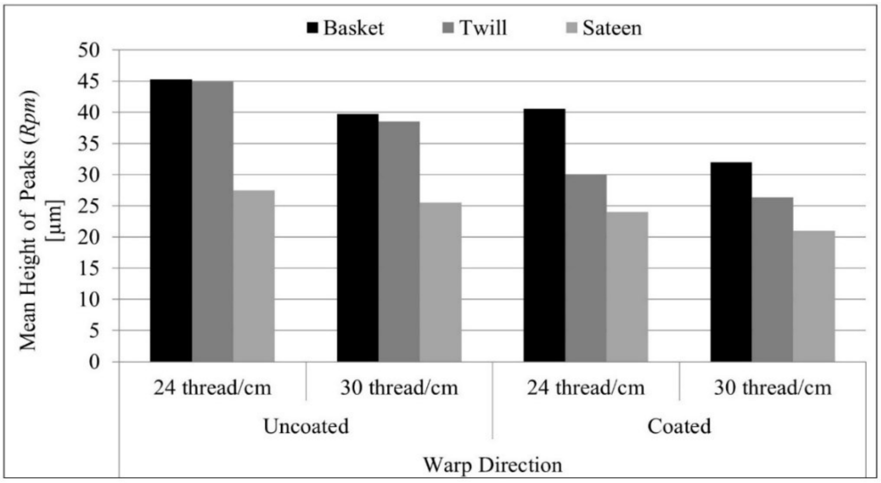

Figure 12. Changes of the mean height of peaks (R_{pm}) values of fabrics in warp direction.

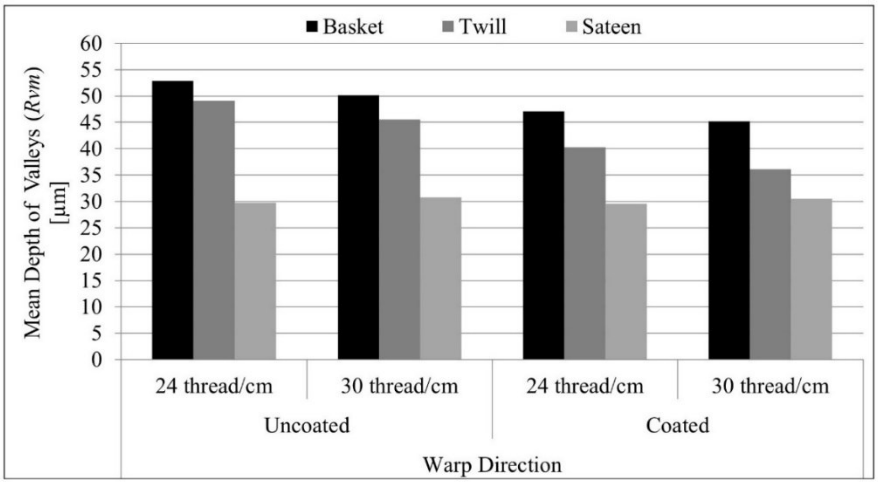

Figure 13. Changes of the mean depth of valleys (R_{vm}) values of fabrics in warp direction.

When the results of uncoated fabrics were examined, the R_{pm} and R_{vm} values of the basket and twill weave fabrics were significantly higher than the sateen weave. Sateen weave fabric had the lowest R_{pm} and R_{vm} values. As can be seen from Figure 4, this might be because the yarns on the surface of the sateen fabric cover the surface more effectively than basket and twill weaves. The long yarn floating might lead to the closeness of yarns in the sateen fabric structure, increase the covering properties of fabrics, and decrease the amplitude of variation in the surface. As a result, the fabric surface roughness decreased.

When the effect of weft yarn density on R_{pm} and R_{vm} values was examined, it was observed that as weft yarn density increased, R_{pm} and R_{vm} values decreased, particularly in basket and twill weave fabrics. The fabric thickness decreased with increasing weft yarn density (Table 3). This was a result of the flattening of the yarns due to the increase in yarn density. The flattened yarns would have led to a compressed fabric thickness and decreased the amplitude of variation in the surface, and as a result, the R_{pm} and R_{vm} values of fabric surfaces decreased.

When the changes in R_{pm} values of fabrics in warp direction after coating were evaluated for weft density values of 24 and 30 threads/cm, respectively, R_{pm} values decreased approximately by 10.37% and 19.52% in basket weave, 33.22%, and 31.61% in twill weave, 12.68% and 17.62% in sateen weave. The lowest change in R_{pm} values occurred in sateen weave base fabric, especially in high weft density values. The highest rate of change was seen on the twill fabric. This was thought to be due to the effect of the diagonal orientation of the yarns in the twill weave structure. In the basket weave, if the high weft density was used, it was seen that the coated fabric gave a low R_{pm} value.

When investigating the changes in R_{vm} values of fabrics in warp direction after coating for weft density values of 24 and 30 threads/cm, respectively, R_{vm} values decreased approximately by 10.95% and 9.84% for basket weave, 17.95% and 20.65% for twill weave and only 0.74% and 0.82% for sateen weave. These findings demonstrated that the R_{vm} values of the fabrics, particularly those with basket and twill weaves, significantly decreased after the coating process. In contrast, the R_{vm} value of the sateen weave fabric surface remained nearly unchanged.

3.3. Evaluation of the fabric surface roughness parameters in weft direction

The changes of the R_a, R_{pm}, and R_{vm} values in the weft direction are shown in Figures 14–16. According to the results, all roughness values of sateen fabric in the weft direction gave the highest values, while it showed the lowest values in the warp direction. It was thought that this result could stem from the deep intersection gaps in the region where the weft yarns were intersected after the long floating over the five warp yarns in the weft direction (Figure 4, Figure 9, and Figure 10). On the surface of the sateen fabric, a group of yarns having long floating in one direction makes the surface more dominant. Therefore, as shown in Figures 4, 9, and 10, the differences in the warp and weft directional yarn settlements caused the variations in roughness parameters to change significantly depending on the fabric direction.

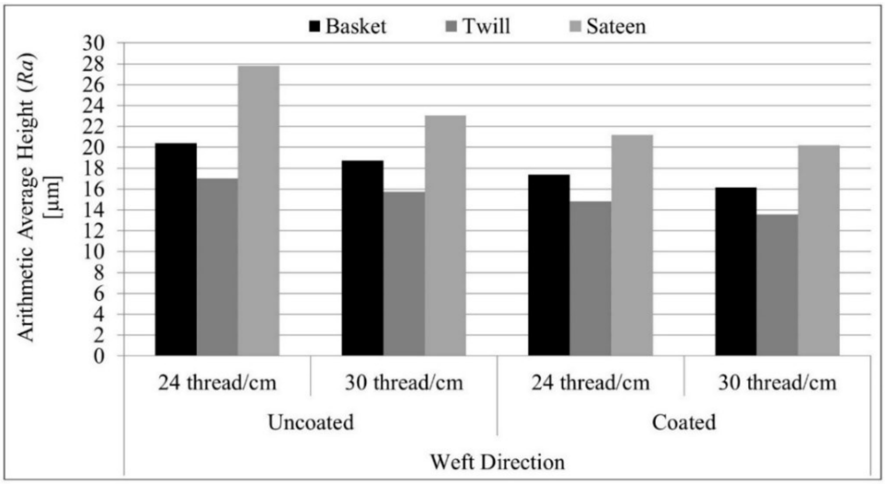

Figure 14. Changes of the arithmetic average height (R_a) values of fabrics in the weft direction.

When the changes in weft direction R_a values of fabrics were analyzed for 24 and 30 threads/cm, respectively, the values decreased by approximately 14.86% and 13.67% in basket weave, 12.92% and 13.73% in twill weave, and 23.93% and 12.43% in sateen weave. In the weft direction, the R_a value of the surface showed the greatest change after the coating process when a sateen weave structure was used on the base, especially with low weft density.

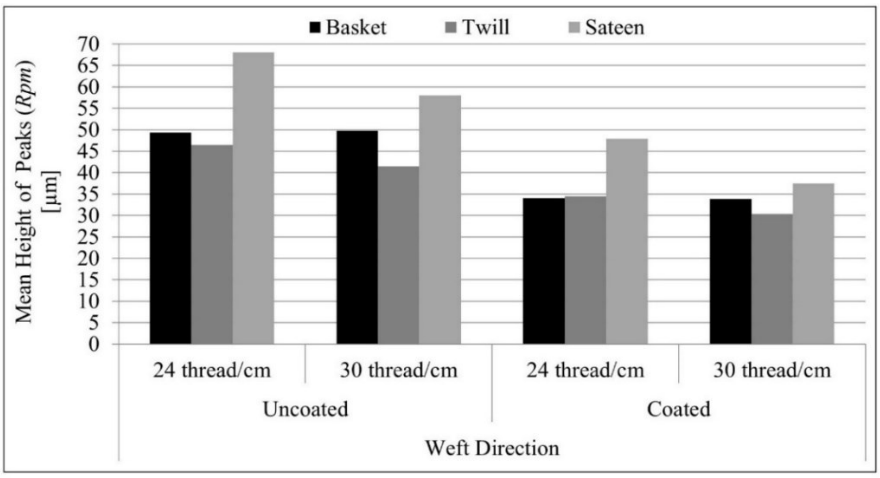

Figure 15. Changes of the mean height of peaks (R_{pm}) values of fabrics in weft direction.

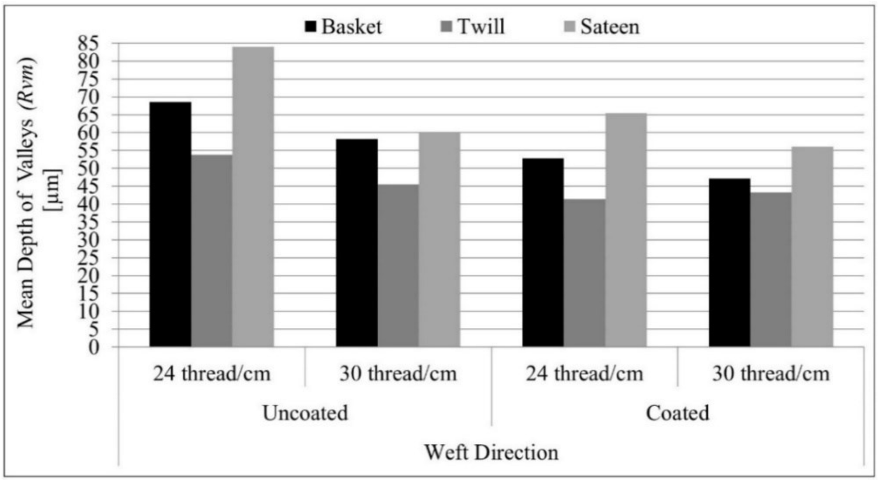

Figure 16. Changes of the mean depth of valleys (R_{vm}) values of fabrics in weft direction.

For weft density values of 24 and 30 threads/cm, R_{pm} values decreased by approximately 30.86% and 32% in basket weave, 25.88% and 26.72% in twill weave, and 29.61% and 35.29% in sateen weave. Similarly, the R_{vm} values showed a decrease of 23.06% and 19.05% in the basket weave, 22.92% and 4.92% in the twill weave, and 22.12% and 6.37% in the sateen weave. Upon examining the changes in R_a, R_{pm}, and R_{vm} values of the fabrics after the coating application, it was revealed that base fabric weave, yarn density, and fabric direction significantly influenced the coated fabric's surface roughness properties.

4. Conclusion

In this study, the effects of different weave patterns of base fabric on the surface roughness parameters of coated polyester fabrics were examined. Experimental results showed that base fabric weave structure was an important parameter affecting the coated fabric's surface roughness. In particular, it was found that the changes in the coated fabric's roughness parameters significantly depend on the fabric's direction. As observed in the sateen weave base fabric, roughness values in the warp direction showed significantly lower values than the other weave structures, while the highest values in the weft direction were obtained. Therefore, it should be considered that the roughness properties of the coated fabric might have different tendencies depending on the fabric's direction. Generally, R_a, R_{pm}, and R_{vm} values of all fabric structures decreased after the coating process. The reduction was more pronounced in surfaces with higher initial roughness values. The findings indicated that weave structures, yarn density, and fabric direction were important parameters to consider when choosing the base fabrics to be coated. This research could help predict how the structural parameters of base fabrics, which were preferred based on their intended use, would influence the surface roughness properties after the coating process.

References

[1] Fung, W., **Coated and laminated textiles**, 416, Woodhead Publishing, Cambridge, (2002).

[2] Shim, E., **Bonding requirements in coating and laminating of textiles** in Jones, I. and Stylios G. K., *Joining Textiles,* Woodhead Publishing, 309-351, Cambridge, (2013).

[3] Billah, S. M. R., **Textile coatings** in Mazumder, M. A., Sheardown, H., Al-Ahmed, A., *Functional Polymers. Polymers and Polymeric Composites: A Reference Series*, Springer, 825-882, (2019).

[4] https://www.mta.gov.tr/v3.0/bilgi-merkezi/kalsit, (14.05.2022).

[5] Mining Specialization Commission, General industrial minerals-1 (Asbestos Graphite- Calcite- Fluorite- Titanium), Technical Report, State Planning Organisation, Ankara, (2001).

[6] Wypych, G., **Handbook of fillers**, 1905, ChemTec Publishing, Toronto, (2016).

[7] Mattila, H. P. and Zevenhoven, R., **Production of precipitated calcium carbonate from steel converter slag and other calcium-containing industrial wastes and residues** in Aresta, M. and Eldik, R. V., *Advances in Inorganic Chemistry,* Academic Press, 347-384, Cambridge, (2014).

[8] Chandran, A. J., Rangappa, S. M., Suyambulingam, I. and Siengchin, S., Micro/nano fillers for value-added polymer composites: A comprehensive review, **Journal of Vinyl and Additive Technology**, 30, 1083-1123, (2024).

[9] Sarkar, A., Ghosh, A. K. and Mahapatra, S., Lauric acid triggered in situ surface modification and phase selectivity of calcium carbonate: its application as an oil sorbent, **Journal of Materials Chemistry***,* 22*,* 11113-11120, (2012).

[10] Fadia, P., Tyagi, S., Bhagat, S., Nair, A., Panchal, P., Dave, H., Dang, S. and Singh, S., Calcium carbonate nano-and microparticles: synthesis methods and biological applications, **3 Biotech**, 11, 1-30, (2021).

[11] Mallick, P. K., **Particulate and short fiber reinforced polymer composites in Kelly, A. and Zweben, C.,** *Comprehensive Composite Materials,* Pergamon, 291-331, Oxford, (2000).

[12] Sun, S., Ding, H., Hou, X., Chen, D., Yu, S., Zhou, H. and Chen, Y., Effects of organic modifiers on the properties of TiO_2-coated $CaCO_3$ composite pigments prepared by the hydrophobic aggregation of particles, **Applied Surface Science**, 456, 923-931, (2018).

[13] Webb, C., Qi, K., Anguilano, L. and Rivera, X. S., Mechanical and environmental evaluation of ground calcium carbonate ($CaCO_3$) filled polypropylene composites as a sustainable alternative to virgin polypropylene, **Results in Materials**, 22, 100562, (2024).

[14] Syafiq, A., Vengadaesvaran, B., Ahmed, U., Abd Rahim, N., Pandey, A. K., Bushroa, A. R., Ramesh, K. and Ramesh, S., Facile synthesize of transparent hydrophobic nano-$CaCO_3$ based coatings for self-cleaning and anti-fogging, **Materials Chemistry and Physics**, 239, 121913, (2020).

[15] Mahmood, N. Q. and Hikmat, M., The effect of calcium carbonate-nanoparticle on the mechanical and thermal properties of polymers utilizing different types of mixing and surface pre-treatment: A review paper, **Engineering and Technology Journal**, 41, 1497-1515, (2023).

[16] Yang, G., Heo, Y. J. and Park, S. J., Effect of morphology of calcium carbonate on toughness behavior and thermal stability of epoxy-based composites. **Processes**, 7, 178, (2019).

[17] Wu, Y., Dai, M., Han, Z., Wang, Y., and Xu, W., Effect of in-situ deposition of nano-calcium carbonate on the properties of anti-creasing cotton fabrics, **Industrial Crops and Products,** 218, 118931, (2024).

[18] Stamboulı, M., Chaouch, W., Gargoubı, S., Zouarı, R. and Msahlı, S., Effect of calcium carbonate particle size and content on the thermal properties of PVC foamed layer used for coated textiles, **Turkish Journal of Chemistry**, 47, 40-46, (2023).

[19] Abeywardena, M. R., Yashomala, M. A. D. H., Elkaduwe, R. K. W. H. M. K., Karunaratne, D. G. G. P., Pitawala, H. M. T. G. A., Rajapakse, R. M. G., Manipura, A. and Mantilaka, M. M. M. G. P. G., Fabrication of water-repellent polyester textile via dip-coating of in-situ surface-modified superhydrophobic calcium carbonate from dolomite, **Colloids and Surfaces A: Physicochemical and Engineering Aspects,** 629, 127397, (2021).

[20] Hou, D., Dai, G., Fan, H., Wang, J., Zhao, C. and Huang, H, Effects of calcium carbonate nano-particles on the properties of PVDF/nonwoven fabric flat-sheet composite membranes for direct contact membrane distillation. **Desalination,** 347, 25-33, (2014).

[21] ISO 21920-2:2021, Geometrical product specifications (GPS)-Surface texture: Profile, Part 2: Terms, definitions and surface texture parameters. **International Organization for Standardization,** (2021).

[22] Thomas, T. R., **Rough surfaces 2nd ed**., 296, Imperial College Press, London, (1998).

[23] Ajayi, J. O., An attachment to the constant rate of elongation tester for estimating surface irregularities of fabrics, **Textile Research Journal**, 64, 8, 475-479, (1994).

[24] Gabrijelčič, H., Colour and optical phenomena on fabric, **Tekstilec**, 50, 4-6, 93-132, (2007).

[25] Zupin, Ž. and Dimitrovski, K., **Mechanical properties of fabrics from cotton and biodegradable yarns bamboo, SPF, PLA in weft** in Dubrovski, P. D., *Woven Fabric Engineering,* IntechOpen, 25-46, Rijeka, (2010).

[26] Ajayi, J. O. and Elder, H. M., Effects of surface geometry on fabric friction, **Journal of Testing and Evaluation**, 25, 2, 182-188, (1997).

[27] Akgun, M., Effect of yarn filament fineness on the surface roughness of polyester woven fabrics, **Journal of Engineered Fibers and Fabrics**, 10, 2, 155892501501000214, (2015).

[28] Akgun, M., The effect of fabric balance and fabric cover on surface roughness of polyester fabrics, **Fibers and Polymers**, 14, 8, 1372-1377, (2013).

[29] Akgun, M., (2014) Surface roughness properties of polyester woven fabrics after abrasion, **The Journal of The Textile Institute**, 105, 4, 383-391, (2014).

[30] Peirce, F. T., 5-The geometry of cloth structure, **Journal of the Textile Institute Transactions**, 28, T45-T96, (1937).

[31] ASTM D3776, Standard test methods for mass per unit area (weight) of fabric, **American Society for Testing and Materials**, (2011).

[32] ASTM D1777-96, Test method for thickness of textile materials, **American Society for Testing and Materials**, (2007).

[33] Gadelmawla, E. S., Koura, M. M., Maksoud, T. M., Elewa, I. M. and Soliman, H. H., Roughness parameters, **Journal of Materials Processing Technology**, 123, 1, 133-145, (2002).

[34] Gupta, K. K., Abbas, S. M. and Abhyankar, A. C., Carbon black/polyurethane nanocomposite-coated fabric for microwave attenuation in X & Ku-band (8-18 GHz) frequency range, **Journal of Industrial Textiles**, 46,2, 510-529, (2016).

[35] Celen, R., Manasoglu, G., Ulcay, Y. and Kanik, M., Usage of barium titanate in fabric coating and investigation of some properties, **Fibers and Polymers**, 22, 1296-1303, (2021).

[36] Manasoglu, G., Celen, R., Akgun, M. and Kanik, M., The effect of graphene coating on surface roughness and friction properties of polyester fabrics, **Materials Science**, 27, 4, 470-476, (2021).

[37] Manasoglu, G., Celen, R. and Kanmaz, D., Improvement of thermal stability, flame retardancy, hydrophobicity, tear and wear performance of polyester fabrics with graphene nanoplatelet coating, **Journal of Applied Polymer Science**, e55765, (2024).